CONCRETE MASONRY UNIT WALLS RETROFITTED WITH ELASTOMERIC SYSTEMS FOR BLAST LOADS

C.F. Johnson*, T.R. Slawson, Ph.D., P.E., T.K. Cummins, J.L. Davis
U.S. Army Engineer Research and Development Center (ERDC)
Vicksburg, MS 39180

ABSTRACT

Concrete masonry units (CMU), commonly referred to as concrete blocks, are the most common construction material utilized throughout the United States and the world for exterior walls of conventional structures. While masonry provides adequate strength for conventional design loads, it does not meet the minimum design standards mandated for blast protection of new and renovated government facilities. One of the most dangerous aspects of blast response is debris hazard, defined as high-velocity fragments originating from walls, windows, light fixtures, equipment, and furniture. Retrofits for conventional structures have evolved over the years from blast hardening through the addition of mass using concrete or steel, to the application of lighter, more resilient and ductile materials. Research at ERDC has focused on the use of elastomeric materials to mitigate debris hazards resulting from blast events.

A series of sub-scale and full-scale experiments was conducted by ERDC to investigate the potential benefit of elastomeric retrofit systems when applied to hollow, unreinforced, CMU walls subjected to an explosive event. This study discusses both the ¼-scale static and dynamic experiments and the full-scale dynamic CMU wall experiments conducted over the past few years. The CMU wall response to static loading was characterized by resistance functions, and normalized pressure and impulse diagrams were used to characterize the dynamic loading.

1. INTRODUCTION

Framed structures with unreinforced CMU infill walls are utilized around the world. While masonry provides adequate strength for conventional design loads, unfortunately, in many circumstances, it is inadequate for meeting the minimum design standards for blast protection of new and renovated structures. These types of walls are extremely vulnerable to blast loads generated from vehicle borne improvised explosive devises (VBIED). The ability of the warfighter to retrofit existing structures in occupied areas to reduce vulnerability against blast loads is of top priority. The increased use of VBIEDs in terrorist attacks around the world over the last few years emphasizes the need to develop retrofit materials and techniques for use on unreinforced CMU walls.

Ideally, blast design would completely prevent human injury, loss of life, structural damage, and property damage, but it is more realistic to try to minimize these hazards and costs. Existing structures must be retrofitted to accommodate cost and time constraints. Conventional retrofit techniques focus on increasing the overall strength of the structure to mitigate the debris hazard by adding steel or concrete. These techniques are difficult to implement, time consuming, expensive, and in some cases, increase the debris hazard. Retrofit techniques that lend ductility to the wall elements instead of strengthening the walls may be more beneficial. The retrofit techniques must accommodate a variety of existing conditions, while incorporating aesthetic considerations and operational requirements. An easily transportable, effective, expedient, and cost-effective retrofit method must be developed.

Over the past 4 years, ERDC has performed over 70 static and dynamic experiments investigating the response of ¼-scale and full-scale CMU walls. ERDC's retrofit materials have evolved from typical conventional materials such as sheet metal, to glass-fiber-reinforced polymers, to new and innovative materials such as spray-on and trowel-on polyureas and thermoplastic films. ERDC researchers have examined materials that would be readily available, lightweight, easily transported and shipped, and easily applied with limited training and equipment needs. This paper will focus on recent results obtained from static and dynamic experiments utilizing elastomeric materials, such as thermoplastic films and trowel-on and spray-on polyureas.

2. WALL CONSTRUCTION

The ¼-scale and full-scale CMU walls were constructed and modeled to represent a simple, unreinforced infill CMU wall. To ensure one-way action, a gap was left between the sides of the CMU wall and the sides of the steel or concrete frame. The first course of blocks in each wall was placed in a mortar bed to provide a simply supported connection. A gap was also used at the top of the wall, with a slip dowel connection to provide lateral support without additional restraint.

Report Documentation Page

Form Approved
OMB No. 0704-0188

1. REPORT DATE	2. REPORT TYPE	3. DATES COVERED
00 DEC 2004	**N/A**	-

4. TITLE AND SUBTITLE	
Concrete Masonry Unit Walls Retrofitted With Elastomeric Systems For Blast Loads	5a. CONTRACT NUMBER
	5b. GRANT NUMBER
	5c. PROGRAM ELEMENT NUMBER
6. AUTHOR(S)	5d. PROJECT NUMBER
	5e. TASK NUMBER
	5f. WORK UNIT NUMBER
7. PERFORMING ORGANIZATION NAME(S) AND ADDRESS(ES) **U.S. Army Engineer Research and Development Center (ERDC) Vicksburg, MS 39180**	8. PERFORMING ORGANIZATION REPORT NUMBER
9. SPONSORING/MONITORING AGENCY NAME(S) AND ADDRESS(ES)	10. SPONSOR/MONITOR'S ACRONYM(S)
	11. SPONSOR/MONITOR'S REPORT NUMBER(S)

12. DISTRIBUTION/AVAILABILITY STATEMENT
Approved for public release, distribution unlimited

13. SUPPLEMENTARY NOTES
See also ADM001736, Proceedings for the Army Science Conference (24th) Held on 29 November - 2 December 2005 in Orlando, Florida., The original document contains color images.

14. ABSTRACT

15. SUBJECT TERMS

16. SECURITY CLASSIFICATION OF:			17. LIMITATION OF ABSTRACT	18. NUMBER OF PAGES	19a. NAME OF RESPONSIBLE PERSON
a. REPORT **unclassified**	b. ABSTRACT **unclassified**	c. THIS PAGE **unclassified**	**UU**	**8**	

2.1 ¼-Scale CMU Wall Construction

The hollow, unreinforced CMU walls used in this study were nominally 64-in. wide by 31-in. tall. The walls were 14-courses tall, and each course was approximately 15.5-blocks wide. The CMU walls were constructed using a ¼-scale replica of a typical 8-in-thick CMU block. The ¼-scale CMU blocks were nominally 2-in. x 4-in. x 2-in. thick and have an average weight of 0.57 lbs. All of the walls used in the static test chamber and most of the walls used in the dynamic tests were constructed on a steel frame that was placed in the test structure. Three of the 11 dynamic walls were selected and tested in a concrete frame to investigate the wall response when applied to a conventional foundation constructed of concrete. Figure 1 presents pictures of the steel and concrete frames used during the ¼-scale experiments.

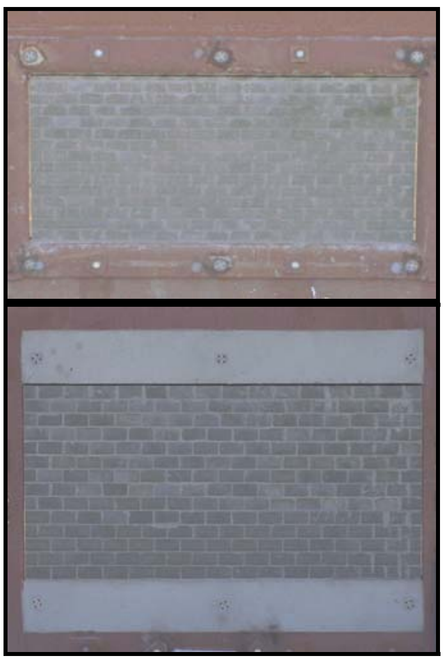

Fig. 1. ¼-scale CMU wall steel and concrete frame.

2.2 Full-Scale CMU Wall Construction

The full-scale CMU walls were constructed in a reinforced concrete frame to replicate a simple, unreinforced, CMU infill wall. Two wall sizes were used in the full-scale experimental series. The first set of walls, nominally 174-in. wide by 111-in. tall, were 14-courses tall and approximately 11 blocks wide. The second set of walls, nominally 224-in. wide x 130-in. tall, were 16-courses tall and 14 blocks wide. The walls were constructed with standard 8-in. x 8-in. x 16-in. CMU blocks with an average weight of 26 lbs. Figure 2 presents pictures of the walls used in the full-scale experiments.

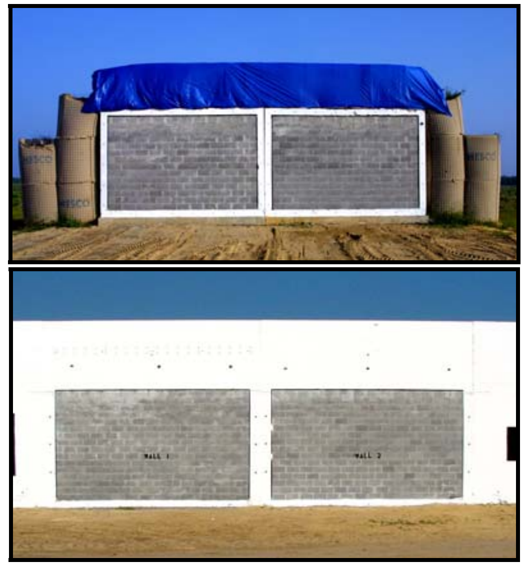

Fig. 2: Full-Scale CMU walls set 1 and 2.

3. WALL RETROFITS

ERDC began the CMU wall retrofit program using conventional materials such as sheet steel. However, recent research has emphasized new and innovative materials, systems, and application procedures focusing on more efficient and economic retrofit systems. The spray-on polyureas required specialized equipment and training for application. Seven different ¼-scale CMU wall retrofit systems were used in the sub-scale static and dynamic experiments and three different full-scale retrofit material systems were selected for validation for a standard threat level.

The first series of CMU walls used a polyurea liner applied at a ¼-scale target retrofit thickness. The first wall (R1) had a spray-on polyurea applied, and the second wall (R2) had a trowel-on polyurea applied. A reinforced polyurea system was selected for the second series of walls. The reinforcement chosen for use was an open weave Aramid fabric. The reinforcement, referred to as a scrim, had varying linear strengths and was used in two different orientations. The scrim orientation used in the selected experiments was defined by the angle the fibers made to the horizontal and vertical axes. For example, the 0/90 scrim lay-up would have fibers at 0 degrees (horizontal) and fibers at 90 degrees (vertical). Similarly, the +/- 45 lay-up would have fibers running in the direction of positive 45 degrees and a fiber in the negative direction 45 degrees to the axes. The third wall (R3) had a spray-on polyurea encompassing a 100-lb-per-linear-in

(pli) scrim applied at a 0/90 degree orientation. The fourth wall (R4) was retrofitted with a spray-on polyurea encompassing a 100-pli scrim applied at a +/- 45 degree orientation. The fifth wall (R5) had a spray-on polyurea encompassing a 200-pli scrim applied at a +/- 45 degree orientation. The final set of wall retrofits were selected because they did not need expensive equipment or specialized training for application. Walls 6 and 7 utilized innovative thermoplastic and polyurethane film materials that could be applied in a technique similar to the application of conventional wallpaper. The sixth wall (R6) had a thermoplastic film applied to the surface of the wall with a spray-on adhesive. The seventh wall (R7) had a polyurethane film applied to the wall surface using an epoxy and tape adhesive system.

4. STATIC EXPERIMENTS

The static test chamber or hydrostatic chamber is one of the key elements used in the retrofitted wall evaluations. Instrumentation for the experiments consisted of three pressure gages and five deflection gages. Two pressure gages were located at the top of the pressurized side of the chamber and one pressure gage was located below the water line on the interior wall of the pressurized side of the chamber. Appropriate corrections to the raw data were made to account for the differential head from the pressurized cavity to the non-pressurized cavity of the chamber. Three deflection gages (D1, D3, D5) were located at the quarter points along the mid-height of the wall, and two deflection gages (D2, D4) placed along the vertical centerline were used to verify one-way action. A video camera and still photography were used to document each experiment. The hydrostatic test chamber and instrumentation plan for the ¼-scale static experiments are shown in Figure 3.

Resistance functions for each CMU wall retrofit system were developed based upon data obtained from the pressure and deflection gages. A resistance function relates the displacement of the element as a load is being applied. The resistance functions developed through the use of most static wall test apparatus, such as vacuum chambers or air bags, are not considered completely accurate beyond the first crack of the CMU wall due to the brittle or dynamic nature of the CMU wall during failure. However, the hydrostatic test chamber, unlike other static loading apparatus, has the ability to capture the post-crack behavior of the retrofitted CMU walls. Therefore, the resistance functions developed by the hydrostatic test chamber are unique, because the complete loading cycle, including the first crack of the CMU wall, failure of the CMU wall, and post-crack behavior including the membrane response are captured. The post crack behavior can be monitored because the hydrostatic chamber allows the pressure to decrease in magnitude once the wall fails until the change in volume or geometric response of the CMU wall and retrofit system equalizes, thereby signifying the wall system's movement into tensile membrane response.

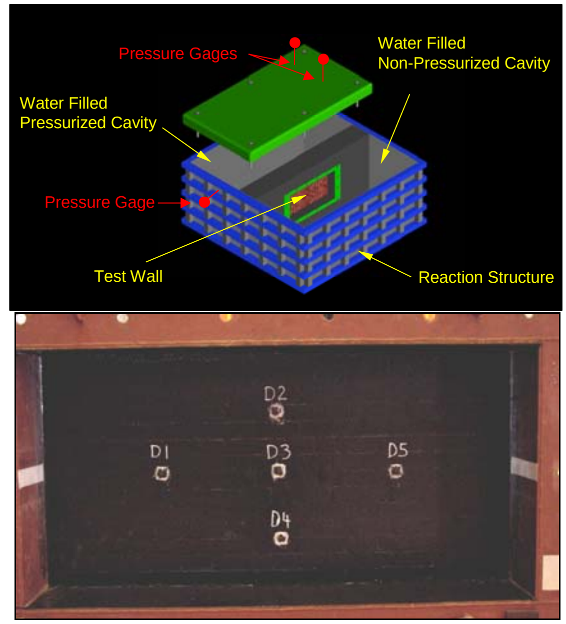

Fig. 3. Hydrostatic chamber and instrumentation plan.

Experimental results obtained from the hydrostatic test chamber demonstrated an increase in ultimate flexural resistance and evaluated the tensile membrane resistance of the retrofitted CMU walls. Existing data from an unretrofitted hollow CMU wall was added as a baseline to demonstrate the existing capacity of the CMU wall and the increase in ductility and strength gained by the retrofit systems. Several key areas on the resistance function can be used to compare and evaluate the retrofit systems. The first area of interest is the wall response at ultimate flexural resistance, which represents the brittle failure of the CMU wall. The second area of interest occurs after the ultimate flexural resistance and represents the transition into tensile membrane response until complete failure of the CMU wall and retrofit system occurs. This information is defined by the maximum pressure and deflection captured by the gages during the experiment. The results from the static test are shown in Table 1 and Figure 4 contains the resistance functions for the baseline wall and the retrofitted wall systems.

As the loading was applied to the retrofitted CMU walls, several different response modes were observed. The first significant response noted was the brittle failure of the CMU wall or ultimate flexural resistance, which is easily recognized on Figure 4 by finding the location of the first peak. Once the CMU wall failed, the magnitude of the pressure decreased until the change in volume or geometric response of the CMU wall and retrofit system

equalized, transitioning the wall system into a tensile membrane response. The wall system was then loaded until ultimate or complete failure of the CMU wall and retrofit system occurred. The increase in ultimate flexural resistance of the retrofit systems over the baseline unreinforced CMU wall is clearly visible in Figure 4.

All of the unreinforced polyurea systems had a similar response during loading except for the spray-on polyurea (R1), which doubled the magnitude of pressure and increased the magnitude of displacement by a factor of 1.5 on average over the other unreinforced polyureas evaluated. The magnitude of pressure at ultimate flexural resistance of the spray-on polyurea wall (R1) was four times higher than the baseline or unretrofitted CMU wall (C1). The trowel-on polyurea (R2), thermoplastic (R6), and polyurethane film (R7) all had very similar pressure and displacement magnitudes varying by only 0.1-in. in

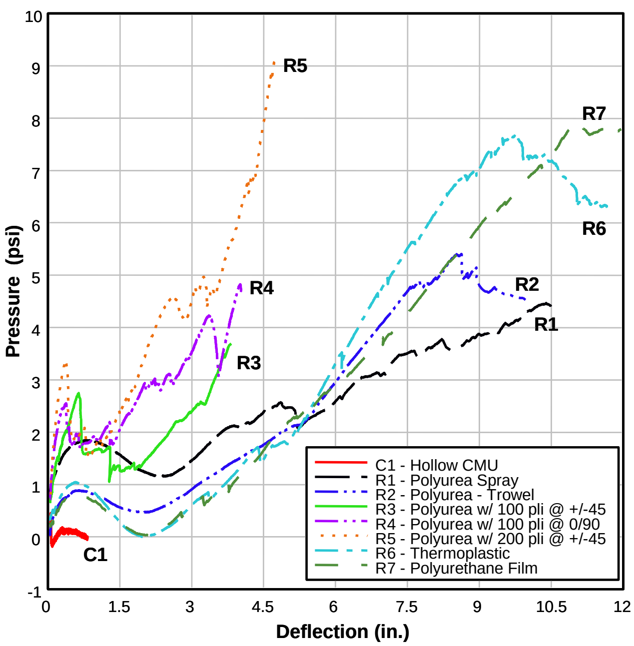

Fig. 4. Resistance functions for hollow unreinforced CMU wall retrofits.

displacement and less than 0.2 psi in pressure between the three and double the pressure of the baseline CMU wall (C1). When comparing the tensile membrane resistance, the polyurethane film (R7) performed very well. R7 deflected over 15-in, the maximum capacity of the static reaction structure, without failing and survived an 8-psi pressure loading. Unfortunately, the neoprene diaphragm used in the static test to administer the hydrostatic load ruptured before R7 failed, so the ultimate response was not obtained. The pressure and displacement magnitudes representing the ultimate flexural resistance and maximum tensile membrane resistance of each wall are listed in Table 1 for comparison.

Table 1. Static Test Results.

Wall	Ultimate Flexural Resistance		Ultimate Tensile Membrane Resistance	
	Pressure psi	Deflection in	Pressure psi	Deflection in
R1	1.845	0.869	4.468	10.397
R2	0.885	0.662	5.407	8.624
R3	2.746	0.642	3.694	3.824
R4	2.548	0.378	4.827	4.012
R5	3.385	0.375	9.198	4.748
R6	1.043	0.566	7.678	9.777
R7	0.845	0.570	8.464	16.989
C1	0.453	0.061	0.453	0.061

As expected, reinforcing the polyurea materials significantly increased the stiffness of the reinforced polyureas compared to the unreinforced polyureas. This increase in stiffness translated into a significant increase in pressure and a decrease in displacement obtained at the ultimate flexural resistance. The tensile strength and orientation of the reinforcement do affect the wall response as seen in Figure 4. It is very interesting to note that the CMU walls with the 100-pli scrim at a 0/90 degree orientation and the 200-pli scrim at a +/-45 degree orientation, believed to be the stiffest materials, both achieved ultimate flexural resistance at the same displacement of 0.375-in. The stronger material (R5) was 1.3 times stronger than the 100-pli (R3) at ultimate flexural resistance, but was six times stronger than R3 at ultimate tensile membrane resistance. When comparing the response of R3 (the 100-pli scrim at a +/-45 degree orientation) and R4 (the 100-pli scrim at a 0/90 degree orientation), the wall with the 0/90 degree orientation had a higher tensile membrane resistance. However, at ultimate flexural resistance, the 0/90 degree orientation (R4) had a higher pressure at a smaller displacement, but the +/- 45 degree orientation (R3) had a higher pressure and displacement. This increase in pressure and displacement could be attributed to the orientation of the scrim in each wall system.

5. DYNAMIC EXPERIMENTS

5.1 ¼-Scale Experiments

The magnitude of the hemispherical charge for each experiment was held constant, and the standoff was selected based upon results obtained from the Wall Analysis Code (WAC) (Slawson, 1995) using the resistance functions obtained in the static experiments. The WAC is a single degree of freedom (SDOF) code used to predict the response of structural elements to blast loads. The final standoff for each dynamic experiment was chosen so that each wall would be subjected to a uniform blast load at a point of imminent failure. The experimental and instrumentation plans used on the ¼-scale dynamic experiments are shown in Figures 5 and 6.

Data recovery consisted of seven blast pressure gages (P1-P6 and F1), two accelerometers (A1, A2), two laser deflectometers (L1, L2), post-test debris distribution, and two high-speed movie cameras. Six pressure gages, P1 through P6, were located around the perimeter of the wall to document the reflected pressure and impulse. The seventh pressure gage, F1, was placed 180 degrees from the wall in a straight line with the charge. The range between the charge and the front face of the wall was also used as the standoff between the charge and the pressure gage, F1. This information was used to document the free-field pressure. Two accelerometers, A1 and A2, were placed at the mid and quarter point to document the wall deflection. Laser L1 at mid-height was used to document the wall's deflection, and laser L2 was used to document the movement at the support.

Fig. 5. ¼-Scale dynamic reaction structure.

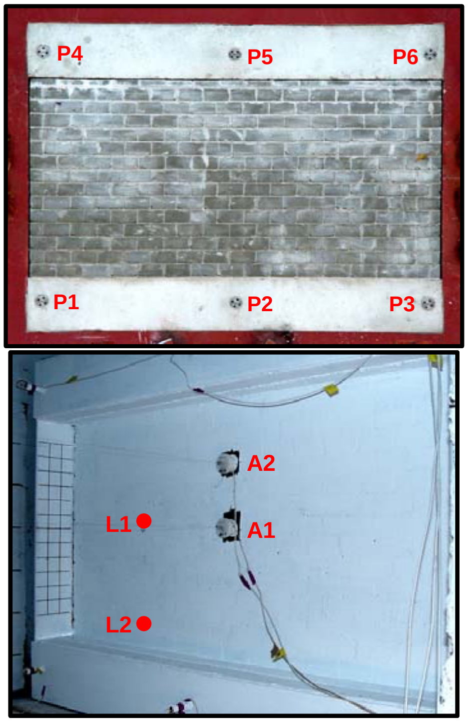

Fig. 6. ¼-Scale dynamic wall instrumentation plan.

The results from the dynamic experiments resemble the response observed in the static experiments. The unreinforced polyureas did add some additional flexural resistance to the hollow unreinforced CMU wall, but the addition of reinforcement to the polyurea retrofit system increased the flexural resistance of the CMU wall significantly. The increase in flexural resistance was directly related to the strength of the reinforcement as well as the orientation of the fibers in the reinforcement material. The ultimate flexural resistance of the unreinforced polyurea retrofits was increased by a factor of 1.4 using the 100-pli scrim at a +/- 45 bias and was doubled by the 200-pli scrim at a +/- 45 bias. Similar to the static experiments, the orientation of the reinforcement appeared to play a significant role in the wall's response. The reinforced polyurea using the 100-pli scrim at a 0/90 bias was too stiff and resulted in a failure at the support, whereas the wall retrofitted with the reinforced polyurea at a +/- 45 scrim bias survived the same dynamic loading. Results from the static experiments suggested that the trowel-on polyurea material (R2) would be weaker than the spray-on polyurea (R1). This was confirmed in the dynamic experiments. The wall retrofitted with the spray-on polyurea (R1) survived, and the wall retrofitted with the trowel-on polyurea (R2) failed under the same loading conditions. Due to the sensitive nature of the data, the values for pressure and impulse have been normalized. The normalized pressure (reflected and incident) and impulse information for each experiment is listed in Table 2. The experimental results for the reflected pressure, P_r, listed in Table 2 represent the average measurements captured by the six pressure gages located on the face of the structure. Figure 7 graphically demonstrates the applicable pressure and impulse ranges listed in Table 2 for each retrofit system based on the charge size used in the experimental program. The individual response of each wall can be seen in Figures 15-20 at the end of the paper.

Table 2. Normalized ¼-Scale Dynamic Results.

Wall	P_r	I_r	P_{so}	I_{so}	Deflection, in
R1	0.42	0.69	0.12	0.23	2.37
R2	0.43	0.70	0.12	0.22	Failed
R3	0.47	0.73	0.16	0.25	2.58
R4	0.47	0.73	0.19	0.26	Failed
R5	0.74	0.89	0.22	0.30	2.50
R6	0.39	0.67	0.12	0.24	2.76

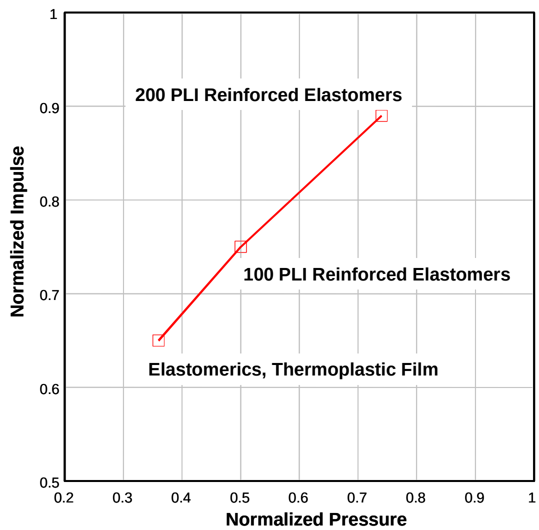

Fig.7. ¼-scale CMU retrofit applicable P-I ranges.

5.2 Full-Scale Experiments

Three of the wall retrofits labeled R8, R9 and R10 in this paper were chosen for full-scale validation. All of the walls were subjected to one standard threat level. The eighth wall (R8) shown in Figure 8 had a spray-on polyurea encompassing an 800-pli scrim applied at a +/-45 degree orientation. The ninth wall (R9) had a full-scale thickness of trowel-on polyurea. The final wall (R10) was built using the trowel-on polyurea as an adhesive for a thermoplastic film applied in a technique similar to the application of conventional wallpaper. See Figures 9 and 10 to see the application procedures for the trowel-on material and thermoplastic film used on walls R9 and R10 respectively.

Fig. 8. R8- Polyurea spray 800 pli @ +/-45.

Data recovery consisted of seven blast pressure gages (P1-P6 and F1), two deflection gages (D1, D2), and one high-speed movie camera. The six pressure gages, P1 through P6, were located around the perimeter of the wall to document the reflected pressure and impulse. The seventh pressure gage, F1, was placed 180 degrees from the wall in line with the charge. The same standoff was used for the CMU wall and the pressure gage F1. This information was used to document the free-field pressure. Two deflection gages, D1 and D2, were placed at the mid and quarter point wall heights to document the wall deflection. See Figure 11 for the full-scale dynamic instrumentation plan.

Fig. 9. R9 – Polyurea trowel-on.

Fig. 10. R10 – Polyurea trowel-on & thermoplastic film.

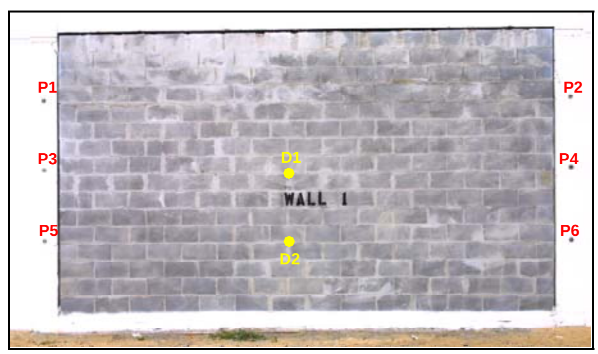

Fig. 11. Full-scale dynamic wall instrumentation.

R8, R9, and R10 performed very well at the full-scale standard threat level. The face shells of most of the walls were destroyed, but the integrity of the retrofit material remained. No debris was found inside any of the reaction structures, which demonstrates the ability of the retrofit systems to mitigate the hazards associated with hollow unreinforced CMU walls. The results have shown that

both spray-on and trowel-on elastomeric retrofit materials and films are effective. See Figures 12, 13 and 14 for post-test views of the walls.

Fig. 12. Post-test view of R8, the spray-on polyurea wall.

Fig 13. Post-test view of R9, the trowel-on polyurea.

Fig. 14. Post-test view of R10, the trowel-on polyurea and film material.

CONCLUSIONS

The results from the static and dynamic experiments showed the increase in ultimate flexural resistance through composite action, as well as the tensile membrane resistance achieved by both unreinforced and reinforced polyurea retrofit systems applied to hollow unreinforced CMU walls. The results from the static experiments indicated that the unreinforced polyurea retrofit systems (R1, R2, R6, and R7) increased the ultimate flexural resistance of the unretrofitted CMU wall by a factor of 1.9 to 4.0, and the reinforced polyurea retrofit systems (R3, R4, and R5) increased the ultimate flexural resistance of the unretrofitted CMU wall by a factor of 5.5 to 7.5. The dynamic experiments indicated similar results between the unreinforced and reinforced polyurea systems. The capacity of the reinforced polyurea retrofit systems was increased by a factor of 1.4 to 2.0 over the unreinforced polyureas, depending on the strength and orientation of the reinforcement.

The full-scale validation proved that the ¼-scale experimental series was effectively used to develop retrofit procedures. The evolution of retrofit materials from conventional materials, such as concrete and steel that took time and equipment, to the first round of elastomeric materials requiring specialized spray equipment and trained labor, to a new area of elastomeric materials that can be applied using a method similar to wallpaper, is very encouraging. As new materials are introduced, the ability to engineer specific retrofits for various threat levels at an efficient or optimum level is increasing. The ability to use a trowel-on polyurea and a thermoplastic film together as a retrofit system without expensive equipment and with minimal training shows that the current research program is evolving quickly to support the current and future needs of the warfighter.

ACKNOWLEDGMENT

The experiments described and the resulting data presented herein were funded by the U.S. Army ERDC, 3909 Halls Ferry Road, Vicksburg, MS 39180-6199. The authors gratefully acknowledge permission from the Director of the Geotechnical & Structures Laboratory and The Chief of Engineers to publish this paper.

REFERENCES

Slawson, T.R., (1995). “Wall Response to Airblast Loads: The Wall Analysis Code (WAC),” prepared for the U.S. Army ERDC, Vicksburg, MS, Contract DACA39-95-C-0009, ARA-TR-95-5208, November, 1995.

DISTRBUTION

Information in this paper is approved for unlimited distribution.

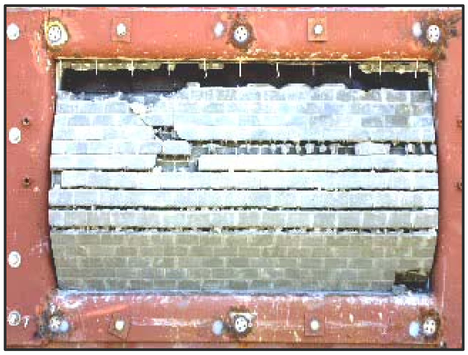

Fig. 15. R1-Polyurea-spray
(P = 0.36, I = 0.65)

Fig. 16. R2-Polyurea-trowel
(P = 0.36, I = 0.65)

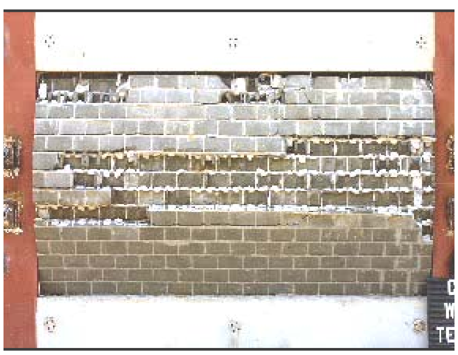

Fig. 17. R3-Polyurea 100 @ +/- 45
(P = 0.5, I = 0.75)

Fig. 18. R4-Polyurea-spray 100 @ 0/90
(P=0.5, I=0.75)

Fig. 19. R5-Polyurea-spray 200 @ +/-45
(P=0.74, I=0.89)

Fig. 20. R6-Thermoplastic film
(P=0.36, I=0.6)